Mitochondrial Respiratory Chain Dysfunction in Dorsal Root Ganglia of Streptozotocin-Induced Diabetic Rats and Its Correction by Insulin Treatment

Subir K. Roy Chowdhury,[1] Elena Zherebitskaya,[1] Darrell R. Smith,[1,2] Eli Akude,[1,2] Sharmila Chattopadhyay,[3] Corinne G. Jolivalt,[3] Nigel A. Calcutt,[3] and Paul Fernyhough[1,2]

OBJECTIVE—Impairments in mitochondrial physiology may play a role in diabetic sensory neuropathy. We tested the hypothesis that mitochondrial dysfunction in sensory neurons is due to abnormal mitochondrial respiratory function.

RESEARCH DESIGN AND METHODS—Rates of oxygen consumption were measured in mitochondria from dorsal root ganglia (DRG) of 12- to- 22-week streptozotocin (STZ)-induced diabetic rats, diabetic rats treated with insulin, and age-matched controls. Activities and expression of components of mitochondrial complexes and reactive oxygen species (ROS) were analyzed.

RESULTS—Rates of coupled respiration with pyruvate + malate (P + M) and with ascorbate + TMPD (Asc + TMPD) in DRG were unchanged after 12 weeks of diabetes. By 22 weeks of diabetes, respiration with P + M was significantly decreased by 31–44% and with Asc + TMPD by 29–39% compared with control. Attenuated mitochondrial respiratory activity of STZ-diabetic rats was significantly improved by insulin that did not correct other indices of diabetes. Activities of mitochondrial complexes I and IV and the Krebs cycle enzyme, citrate synthase, were decreased in mitochondria from DRG of 22-week STZ-diabetic rats compared with control. ROS levels in perikarya of DRG neurons were not altered by diabetes, but ROS generation from mitochondria treated with antimycin A was diminished compared with control. Reduced mitochondrial respiratory function was associated with downregulation of expression of mitochondrial proteins.

CONCLUSIONS—Mitochondrial dysfunction in sensory neurons from type 1 diabetic rats is associated with impaired rates of respiratory activity and occurs without a significant rise in perikaryal ROS. *Diabetes* **59:1082–1091, 2010**

Peripheral nerves of diabetic patients develop a spectrum of pathology that can take many years to emerge (1,2). Experimental studies over shorter time periods have demonstrated that hyperglycemia can induce cellular damage through increased glucose metabolism by aldose reductase (3), elevated protein glycation (4), and increased mitochondrial NADH supply, which enhances electron availability causing partial reduction of oxygen to superoxide radicals in the proximal part of the electron transport chain (5,6). These three mechanisms may combine to trigger large elevations in reactive oxygen species (ROS) that induce oxidative stress and tissue damage (7–9). The ability of nerves to survive oxidative stress may also be impaired in diabetes because of suboptimal trophic support from insulin, insulin-like growth factors, and neurotrophic factors (10,11).

Although increased oxidative stress has become a widely accepted consequence of hyperglycemia in models of diabetic neuropathy, the source of excessive ROS is not defined. Mitochondria are one plausible source of ROS, based on reports of an acute glucose-induced elevation of flux through the electron transport chain in endothelial cells that was accompanied by hyperpolarization of the mitochondrial inner membrane and subsequent stimulation of ROS generation in the proximal aspect of the electron transport chain (5,6). However, this mechanism may not extend to other cell types or to longer durations of diabetes, since mitochondrial respiration and enzymatic activities are reduced in mitochondria from streptozotocin (STZ)-induced diabetic rat hearts (12,13), and activity of the mitochondrial electron transport chain and citrate synthase are decreased in skeletal muscle of patients with type 2 diabetes (14–16). Further, we and others have measured depolarization, rather than hyperpolarization, of the mitochondrial inner membrane in acutely isolated adult DRG sensory neurons from STZ-diabetic rats that can be corrected by treatment with neurotrophin-3 or insulin at doses that did not affect hyperglycemia (17–19). Given the unclear understanding of the contribution of mitochondrial-derived ROS to neuronal oxidative stress, we have now directly measured rates of activity within the mitochondrial respiratory chain and ROS production in neurons from STZ-diabetic rats.

RESEARCH DESIGN AND METHODS

Induction, treatment, and confirmation of type 1 diabetes. Male Sprague-Dawley rats were made diabetic with a single intraperitoneal injection of 75 mg/kg STZ (Sigma, St. Louis, MO). These diabetic rats were healthy and did not need insulin supplementation to maintain body weight. Insulin

TABLE 1
Rat body weight, blood glucose levels, and glycated hemoglobin at end point

	n	Weight (g)	Blood glucose (mmol/l)	A1C (%)
Cohort 1 (12 weeks)				
Control	5	603.7 ± 38.8****	8.14 ± 1.52****	4.34 ± 0.24****
Diabetic	5	280.4 ± 16.5	28.16 ± 3.53	7.70 ± 0.78
Cohort 2 (16 weeks)				
Control	11	679.4 ± 25.3****	8.80 ± 2.34****	4.76 ± 0.21****
Diabetic	7	367.7 ± 42.5	31.09 ± 2.96	8.90 ± 0.73
Cohort 3 (22 weeks)				
Control	6	756.17 ± 70.03*	8.25 ± 0.85*	3.48 ± 0.10*
Diabetic	6	413.25 ± 64.30	30.72 ± 1.65	7.76 ± 0.77
Diabetic + insulin	6	498.97 ± 24.02***	20.37 ± 11.11***	7.32 ± 0.61
Cohort 4 (22 weeks)				
Control	12	782.73 ± 107.39*	8.29 ± 1.58*	4.65 ± 0.38*
Diabetic	12	390.13 ± 43.72	29.03 ± 2.63	10.68 ± 1.04
Diabetic + insulin	12	493.30 ± 50.38**	20.23 ± 6.85	9.10 ± 0.65**

Starting body weight ranged between 275 and 325 g. Cohorts were maintained for 12–22 weeks. Rats from cohort 3 and 4 were used for the preparation of lumbar DRG tissue homogenate samples and isolated mitochondria samples from lumbar DRG, respectively. Values are means ± SD. *$P < 0.05$ vs. other groups; **$P < 0.001$ vs. diabetic; ***$P < 0.05$ vs. diabetic (all by one-way ANOVA with Tukey's post hoc test); and ****$P < 0.0001$ vs. diabetic (Student's t test). Note that %A1C values in cohort 3 were derived using the DCA 2000 + kit ($n = 4$–5) and for cohort 4 were generated using the A1C Now kit ($n = 8$–11).

implants (two Linplant implants; Linshin Canada, Toronto, ON, Canada) were placed subcutaneously into a subgroup of STZ-diabetic rats after 18 weeks of diabetes and remained in place for a further 4 weeks to test the impact of suboptimal insulin levels on mitochondrial function. Animals were killed and tissue collected after 12, 16, or 22 weeks of diabetes. Animal procedures followed guidelines laid down by the University of Manitoba Animal Care Committee using the Canadian Council of Animal Care guidelines. Nonfasting blood glucose concentration was measured using the Accu-Chek Compact Plus glucometer (Roche, Laval, QC, Canada) and blood A1C levels by the A1cNow+ system (Bayer Healthcare, Sunnyvale, CA). Nerve sugar and polyol content was measured by gas chromatography of trimethylsilyl derivatives (17) and lipid peroxidation by spectrophotometric assay of total malondialdehyde (MDA) and 4-hydroxyalkanal (HAE) content (LPO-586 kit, Oxis, CA) (20).

Preparation of tissue homogenates and isolated mitochondria from lumbar DRG. Cohorts 1, 2, and 3 (Table 1) were used to prepare lumbar DRG tissue homogenates for mitochondrial respirometry, and another group (cohort 4) was used as a source of mitochondrial preparations from lumbar DRG. Lumbar DRG were rinsed in ice-cold solution containing sucrose/Tris/EDTA (STE) buffer (250 mmol/l sucrose, 10 mmol/l Tris-HCl, 1 mmol/l EDTA, pH 7.4) and then homogenized with a polytron homogenizer (Kinematica, Lucerne, Switzerland) using 3 × 7.5 s grinding pulses at 30-s intervals. In cohort 4, mitochondria were isolated from lumbar DRG using a differential centrifugation method (21). The protein content was measured according to the method of Bradford. The degree of integrity of the mitochondrial preparation was tested by adding exogenous cytochrome c (10 μmol/l) in the presence of pyruvate, malate, and ADP. Under these conditions, the respiration rate in lumbar DRG was increased by 17 ± 8% in control and 22 ± 9% in 22 weeks STZ-diabetic rats (means ± SD, $n = 4$). This demonstrates a low level of fragmentation of the mitochondria and the similarity of the preparation between the two groups.

Western blotting for mitochondrial proteins. Mitochondrial preparations were homogenized in STE buffer and 5–10 μg protein resolved on a 10% SDS-PAGE gel and electroblotted onto nitrocellulose membrane. Blots were then blocked in 5% nonfat milk containing 0.05% Tween-20, rinsed in PBS (pH 7.4), and incubated with the following antibodies: monoclonal anti–cytochrome c oxidase subunit 4 (COX IV, 1:1,000; MitoSciences, Eugene, OR), monoclonal anti-NADH dehydrogenase (ubiquinone) iron-sulfur protein 3 (NDUFS3, 1:1,000; MitoSciences), and monoclonal anti-ATP synthase β subunit (1:2,000 dilution; MitoSciences). Extracellular signal–regulated kinase (ERK, 1:2,000; Covance) was probed as a loading control (previous studies show this protein to not change level of expression in DRG in diabetes). The blots were rinsed, incubated in Western blotting Luminol Reagent (Santa Cruz Biotechnology), and imaged using a Bio-Rad Fluor-S image analyzer (Bio-Rad, Hercules, CA).

Mitochondrial respiration assay. Oxygen consumption was determined at 37°C using the OROBOROS Oxygraph-2K (OROBOROS Instruments, Innsbruck, Austria) (22). Tissue homogenates or isolated mitochondria from lumbar DRG were resuspended in KCl medium (80 mmol/l KCl, 10 mmol/l Tris-HCl, 3 mmol/l MgCl$_2$, 1 mmol/l EDTA, 5 mmol/l potassium phosphate, pH 7.4). Various substrates and inhibitors for mitochondrial respiratory chain complexes were used as described in Fig. 1. OROBOROS DatLab software was used to calculate the oxygen consumption.

Determination of enzymatic activities of mitochondrial complexes and citrate synthase. All measurements of enzymatic activities in lumbar DRG mitochondrial preparations were performed spectrophotometrically using a temperature-controlled Ultrospec 2100 ultraviolet-visible spectrophotometer (Biopharmacia Biotech, Uppsala, Sweden). Complex I activity was measured as rotenone-sensitive NADH:cytochrome c reductase activity. Purified mitochondria were thawed and subjected to three freeze-thaw cycles to disrupt mitochondrial membranes and permit access of substrates. Freshly prepared assay buffer (50 mmol/l K-phosphate, pH 7.4, 1 mmol/l potassium cyanide (KCN), 100 μmol/l NADH) and 10 μg protein of mitochondrial preparation were added to the cuvette and preincubated for 3 min at 25°C. After addition of 100 μmol/l oxidized cytochrome c, the reaction was followed for 2 min at 550 nm and then for 2 more minutes after addition of 25 μmol/l rotenone to allow calculation of the rotenone-sensitive complex I activity. Complex IV activity was measured at 25°C by monitoring the absorbance decrease of reduced cytochrome c at 550 nm (23). The reaction was started by addition of 40 μmo/l reduced cytochrome c into 50 mmol/l phosphate buffer containing 5 μg mitochondrial protein solubilized with 0.02% laurylmaltoside. Activity of the Krebs cycle enzyme, citrate synthase, was determined at 25°C in medium containing 150 mmol/l Tris-HCl (pH 8.2), 0.02% laurylmaltoside, 0.1 mmol/l dithionitrobenzoic acid, and 5 μg mitochondrial protein (24). The reaction was initiated by addition of 100 μmol/l acetyl CoA and changes in absorbance at 412 nm were measured for 1 min. This value was subtracted from the rate obtained after addition of 0.05 mmol/l oxaloacetic acid.

Analysis of ROS measurement in adult sensory neurons. Adult lumbar DRG sensory neuron cultures from age-matched control and 22-week STZ-diabetic rats were prepared as described previously (17). Neurons were suspended in modified Bottenstein and Sato's N2 medium (0.1 mg/ml transferrin, 20 nmol/l progesterone, 100 μmol/l putrescine, 30 nmol/l sodium selenite, and 1 mg/ml BSA, 0.01 mmol/l cytosine arabinoside; all from Sigma) in Ham's F12. To mimic in vivo conditions, the following additions were made to the basal defined medium: control 10 nmol/l insulin and diabetic 25 mmol/l glucose. ROS levels were imaged on a Carl Zeiss LSM510 inverted confocal microscope using two dyes: dihydrorhodamine 123 (DHR123) or 5-(and-6)-chlromethyl-2′7′-dichlorohydrofluorescein diacetate acetyl ester (CM-H$_2$DCFDA). Neurons were loaded with 5 μmol/l DHR 123 (Sigma, in 100% stock solution) or 1.2 μmol/l CM-H$_2$DCFDA (Invitrogen, Carlsbad, CA) for 30 or 15 min, respectively, at 37°C. For DHR 123 and CM-H$_2$DCFDA, excitation/emission was 488/>505 nm.

Measurement of ROS in mitochondrial preparations from lumbar DRG. ROS generation in lumbar DRG mitochondria from control and 22-week STZ-diabetic rats was evaluated by the detection of H$_2$O$_2$. Hydrogen peroxide production was determined fluorometrically by measuring oxidation of Amplex Red (Invitrogen) (22). Fluorescence of the Amplex Red oxidation product was measured at 25°C using SpectraMax Gemini spectrofluorometer (Molecular Devices, Sunnyvale, CA). Excitation/emission wavelengths were 530/590 nm. The assay was performed with 100 μg mitochondrial protein per
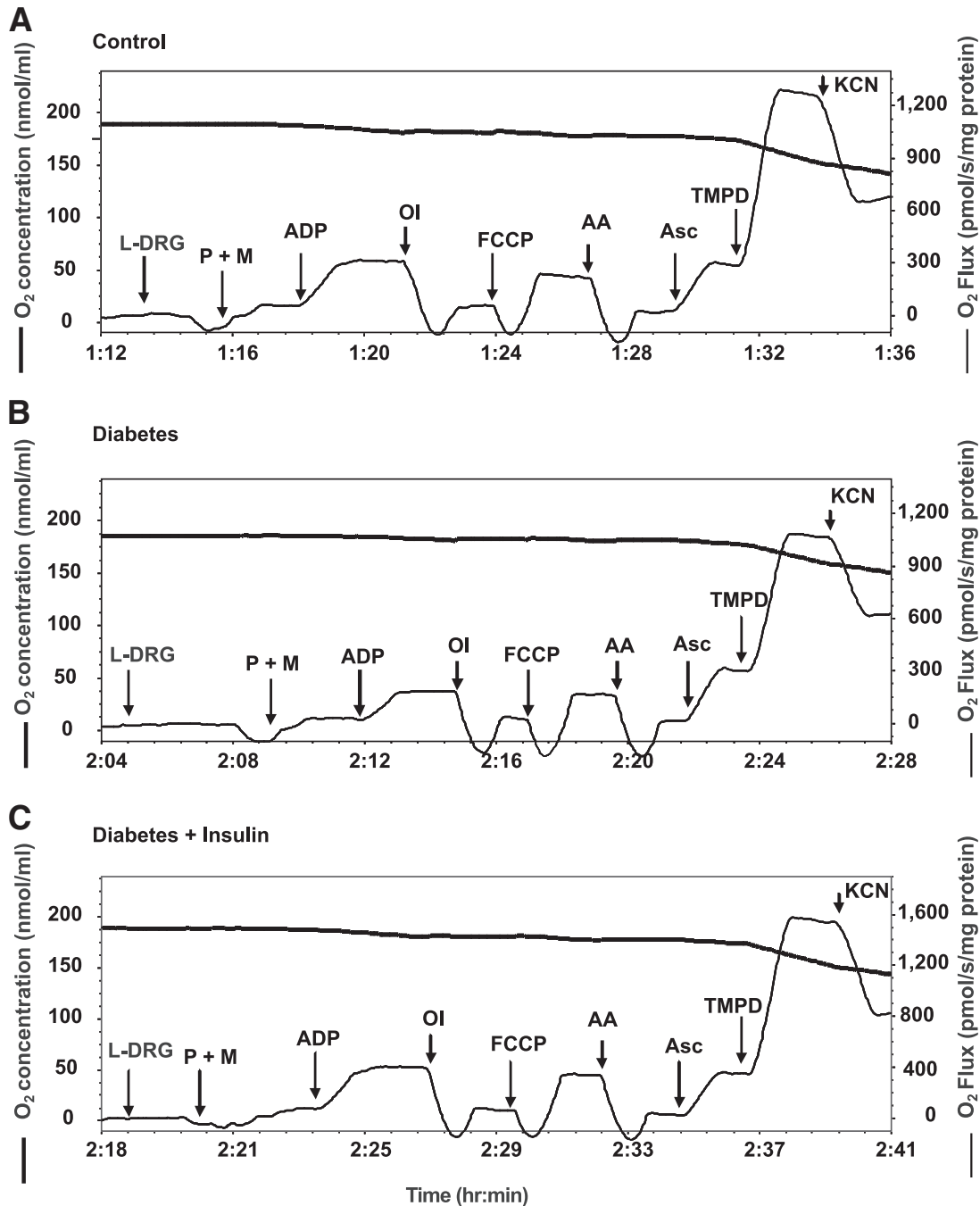
FIG. 1. Representative measurements of oxygen consumption in isolated lumbar DRG mitochondria from control, diabetic, and insulin-treated diabetic rats. Freshly isolated lumbar DRG mitochondria were assessed in control (A), diabetic (B), and insulin-treated (C) diabetic rats using OROBOROS oxygraph 2K as described in RESEARCH DESIGN AND METHODS. Thick lines indicate the level of oxygen in the chamber of electrode and expressed in nanomoles per milliliter. Thin lines indicate oxygen flux per mass (picomoles O_2 per second per milligram protein) in the presence of specific substrates and inhibitors of the mitochondrial respiratory chain. L-DRG, lumbar dorsal root ganglia mitochondria; P, pyruvate (10 mmol/l); M, malate (5 mmol/l); ADP, adenosine diphosphate (2 mmol/l); OI, oligomycin (1.0 μmol/l); FCCP, carbonyl cyanide 4-trifluoromethoxy-phenylhydrazone (0.5 μmol/l); AA, antimycin A (1 μg/ml); Asc, ascorbate (5 mmol/l); TMPD, N,N,N′,N′-tetramethyl-p-phenylenediamine dihydrochloride (0.5 mmol/l); KCN, potassium cyanide (0.25 mmol/l).

milliliter in KCl-based medium supplemented with 10 mmol/l pyruvate and 5 mmol/l malate in the presence or absence of antimycin A (10 μg/ml). Amplex red was used at 50 μmol/l, with horseradish peroxidase at 0.5 units/ml.

Nerve structure and function. Function of small sensory neurons was inferred by measuring hind paw thermal response latency using a modified Hargreaves apparatus (University Anesthesia Research and Development, San Diego, CA) with a heating rate of ~1°C/s from a baseline of 30°C and with a cutoff at 20 s (25). The structural integrity of small sensory neurons was assessed by measuring intraepidermal nerve fiber (IENF) profiles in hind paw plantar skin that was immersion fixed in 4% paraformaldehyde and processed to paraffin blocks. Sections (6 μm) were stained with the pan-neuronal marker

PGP9.5 (1:1,000; Biogenesis, U.K.) and viewed under a light microscope to allow counting of IENF and subepidermal nerve profiles per unit length of the dermal:epidermal border (26). Structural integrity of large myelinated fibers was assessed by measuring mean axonal caliber in distal tibial nerves that were immersion fixed in 2.5% glutaraldehyde, postfixed in osmium tetroxide, and processed to araldite blocks before cutting 1.0-μm sections. Tissue sections were stained with p-phenylenediamine and viewed under a light microscope connected to a computer running image analysis software to allow calculation of axonal diameter (17).

Data analysis. Where appropriate, data were subjected to one-way ANOVA with post hoc comparison using Tukey's test or two-way ANOVA with Bonferroni's

TABLE 2
Sugar, protein, and lipid peroxidation levels in sciatic nerve

	Glucose (nmol/mg) dry weight	Fructose (nmol/mg) dry weight	*myo*-Inositol (nmol/mg) dry weight	Total protein (mg/cm)	MDA + HAE (nM/mg) wet weight
Control	Nd	Nd	13.24 ± 3.05	1.10 ± 0.24**	12.67 ± 2.36
Diabetic	33.3 ± 9.66**	8.89 ± 6.08	7.94 ± 1.24*	0.98 ± 0.23**	17.35 ± 0.79*
Diabetic + Ins	16.98 ± 8.37	7.55 ± 3.73	11.2 ± 5.8	1.42 ± 0.40*	16.59 ± 3.81*

Sciatic nerves were taken from cohort 4. Values are means ± SD ($n = 6$–9). *$P < 0.05$ vs. control; **$P < 0.05$ vs. diabetic + insulin. Sorbitol levels were too low to detect in all samples. Nd = nondetectable.

post hoc tests (GraphPad Prism 4; GraphPad Software, San Diego, CA). In all other cases, standard two-tailed Student's *t* test was performed.

RESULTS

STZ-diabetic rats did not suffer weight loss during the study but showed reduced weight gain after 12–22 weeks of STZ-induced diabetes compared with age-matched controls (Table 1). Persistence of diabetes was also indicated by elevated nonfasting blood glucose and glycated hemoglobin levels (Table 1). STZ-diabetic rats of cohorts 3 and 4 that received insulin supplementation for the final 4 weeks of a 22-week period of diabetes showed a partial recovery of body weight accompanied by a partial decrease in blood glucose, but retained elevated glycated hemoglobin levels. Insulin treatment also partially lowered nerve glucose content and corrected the deficit in *myo*-inositol (Table 2). Diabetes-induced increases in nerve fructose content and lipid peroxidation were not altered by insulin therapy. Nerve protein content was not altered by diabetes, whereas insulin treatment significantly increased this parameter above in both controls and untreated diabetic rats.

There was no overt evidence of degeneration in the distal tibial nerve of rats after 22 weeks of diabetes (supplemental Fig. 1A and B, available in an online appendix at http://diabetes.diabetesjournals.org/cgi/content/full/db09-1299/DC1), and morphometric analysis indicated a mild trend toward decreased mean axonal diameter associated with a shift in the size-frequency distribution toward smaller fibers (supplemental Fig. 1C and D). Paw thermal response latency was normal in rats after 22 weeks of diabetes, as were both IENF and subepidermal nerve profile counts (supplemental Fig. 2A–D). Insulin supplementation for the last 4 weeks of diabetes significantly increased paw IENF profile number compared with controls (supplemental Fig. 2D).

Mitochondrial respiratory chain activity of DRG was determined using a Clarke type electrode in the presence of specific substrates and inhibitors of the mitochondrial respiratory chain. Figure 1 demonstrates typical measurements of oxygen consumption in freshly isolated mitochondria of lumbar DRG from age-matched control, diabetic, and insulin-treated diabetic rats. Basal respiration in lumbar DRG mitochondria is stated as respiration at state 4 with energetic substrates, pyruvate and malate (P + M). Coupled respiration at state 3 was induced by addition of ADP. After this measurement, the ATP-synthase specific inhibitor, oligomycin (Ol), was added to prevent reverse pumping of protons by the ATPase, and then the uncoupled rate was determined by adding the uncoupling agent, carbonylcyanide p-trifluoromethoxyphenylhydrazone (FCCP). Uncoupled respiration was inhibited at complex III by antimycin A. Ascorbate (Asc) and N,N,N′,N′-tetramethyl-p-phenylenediamine (TMPD) were

then added to determine the capacity of cytochrome *c* oxidase (complex IV). TMPD is an artificial redox mediator that assists transfer of electrons from ascorbate to cytochrome *c*. Complex IV respiration was calculated as
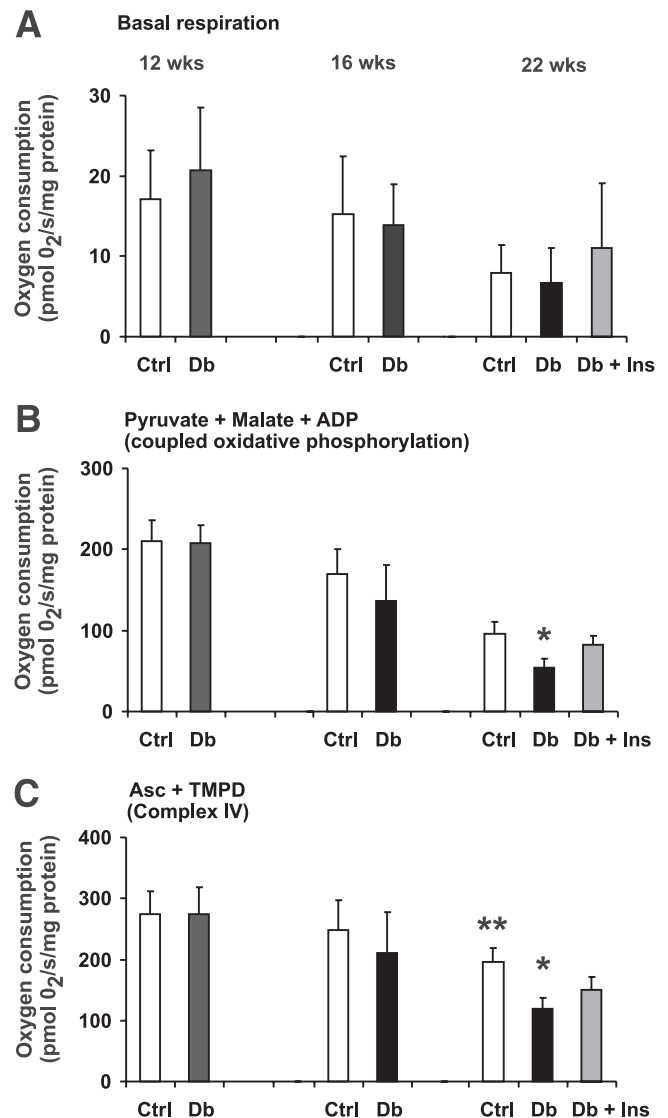

FIG. 2. Effect of 12–22 weeks of STZ-induced diabetes on the activity of the mitochondrial respiratory chain in freshly prepared lumbar DRG tissue homogenate. Measurements of oxygen consumption were performed with energetic substrates, pyruvate and malate, as described in Fig. 1. Basal respiration (*A*), pyruvate + malate + ADP (coupled oxidative phosphorylation) (*B*), and the respiration rate with Asc + TMPD (complex IV) (*C*) were assessed in age-matched controls (Ctrl), STZ-diabetic rats (Db), and STZ-diabetic rats with insulin implant (Db + Ins) at 12 ($n = 5$), 16 ($n = 7$–11), and 22 ($n = 5$–6) weeks of diabetes. Values are means ± SD; n = as indicated. *$P < 0.05$ vs. Db + Ins; **$P < 0.001$ vs. Db (one-way ANOVA with Tukey's post hoc comparison).
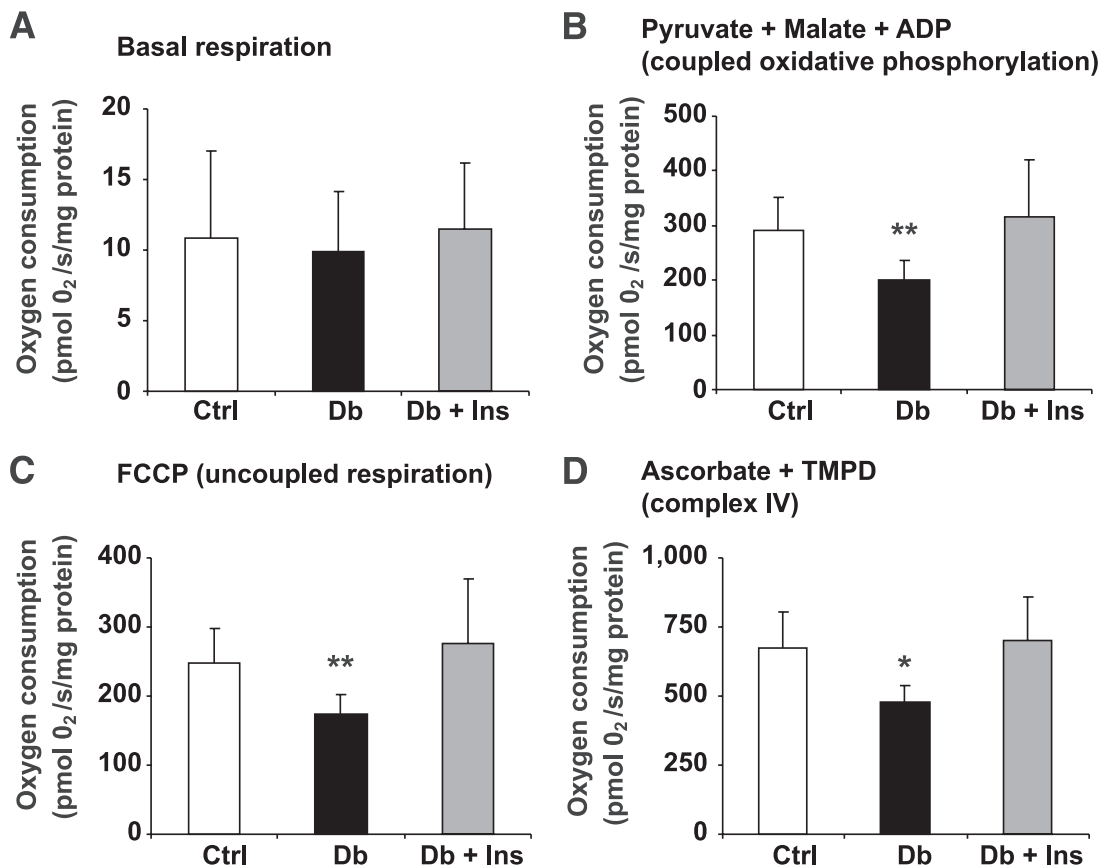
FIG. 3. Mitochondrial respiratory chain activity is impaired in freshly isolated mitochondria from lumbar DRG of 22 weeks of STZ-diabetic rats. After measurement of coupled respiration, the ATP synthase specific inhibitor, oligomycin, was added to prevent reverse pumping of protons by the ATPase, and then the uncoupled rate of mitochondrial respiration was generated by adding the uncoupling agent FCCP. Basal respiration (*A*), pyruvate + malate + ADP (coupled oxidative phosphorylation) (*B*), FCCP (uncoupled respiration) (*C*), and the respiration rate with Asc + TMPD (complex IV) (*D*) were measured in age-matched controls (Ctrl), STZ-diabetic rats (Db), and STZ-diabetic rats with insulin implant (Db + Ins) after 22 weeks of diabetes. Values are means ± SD, $n = 6$. *$P < 0.05$ vs. other groups; **$P < 0.05$ vs. Db + Ins (one-way ANOVA with Tukey's post hoc comparison). Treatment of the mitochondrial preparation with the uncoupler FCCP induced a four- to sixfold elevation in the rate of oxygen consumption over the basal rate confirming that the mitochondrial preparations were intact and of high quality in all groups.

the portion sensitive to KCN, a specific inhibitor of cytochrome *c* oxidase.

Basal respiration with pyruvate and malate (P + M), rates of coupled respiration at state 3, and the respiration rate with ascorbate and TMPD (Asc + TMPD; complex IV) of lumbar DRG tissue homogenates from control and STZ-diabetic rats were not changed after 12 weeks of diabetes (Fig. 2). After 16 weeks of diabetes, there was a statistically nonsignificant decrease in coupled respiration and the respiration rate with Asc + TMPD in STZ-diabetic rats. With progression of untreated diabetes to 22 weeks in both lumbar DRG tissue homogenates (Fig. 2*B*) and isolated mitochondria from lumbar DRG (Fig. 3*B*), coupled respiration with P + M was decreased by 31–44% in diabetic rats compared with control lumbar DRG tissue. This attenuated mitochondrial respiratory activity was significantly improved by 4 weeks of insulin treatment. Respiration rates with Asc + TMPD were decreased by 29–39% in diabetic lumbar DRG tissues and mitochondrial preparations and protected by insulin (Figs. 2*C* and 3*D*). Uncoupled respiration in mitochondria isolated from lumbar DRG was also decreased in STZ-diabetic rats compared with control and significantly improved by insulin supplementation (Fig. 3*C*). These deficits were specific for lumbar DRG, since similar measurements in cortex revealed no effect after 22 weeks of diabetes (supplemental Table 1).

Enzymatic activities of mitochondrial complexes and the Krebs cycle enzyme, citrate synthase, were assessed in mitochondria isolated from lumbar DRG of age-matched control and 22-week STZ-diabetic rats. The activity of mitochondrial complex I was assessed as rotenone-sensitive NADH-cytochrome *c* reductase when cytochrome *c* is the acceptor of electrons. The enzymatic activities of rotenone-sensitive NADH-cytochrome *c* reductase (complex I) and cytochrome *c* oxidase (complex IV) as well as the Krebs cycle enzyme, citrate synthase, were significantly decreased in STZ-diabetic rats compared with control (Fig. 4).

To determine if decreased mitochondrial activity in diabetic animals was associated with alterations in ROS generation, adult sensory neurons from lumbar DRG were cultured from age-matched control and STZ-diabetic rats and assessed within 2 h of plating for levels of ROS using the fluorescent dyes DHR 123 and CM-H_2DCFDA. Both dyes provide a broad readout of a range of ROS. Figure 5*A*–*C* show that sensory neurons from all treatment groups exhibited similar levels of DHR 123 fluorescence emission from perikarya. In a separate group of STZ-diabetic rats, ROS levels in acutely isolated neurons were detected using CM-H_2DCFDA and confirmed the lack of any effect of diabetes on ROS generation (Fig. 5*D*–*F*). ROS generation (H_2O_2 as detected by Amplex red) by mitochondria isolated from lumbar DRG of age-matched

A Rotenone-sensitive NADH-cytochrome c reductase

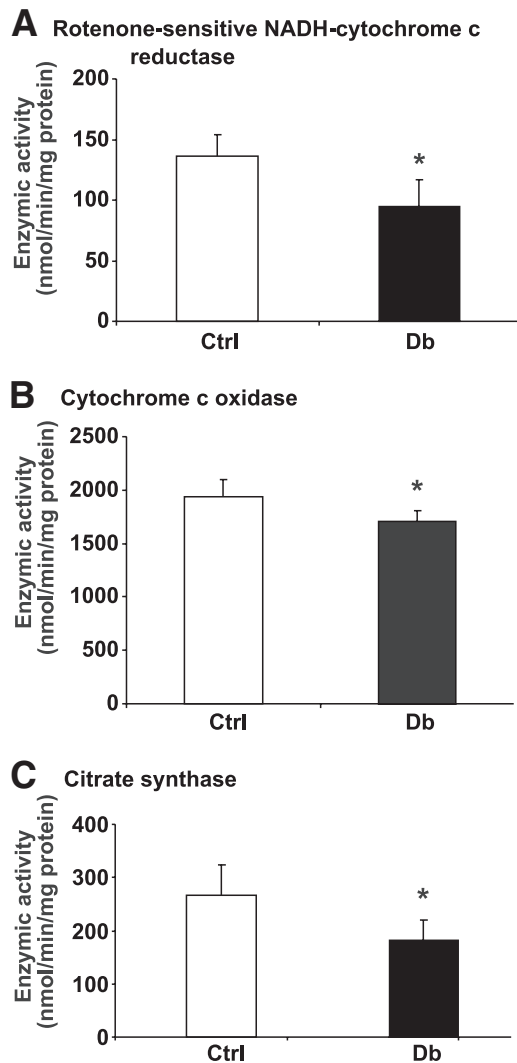## B Cytochrome c oxidase

C Citrate synthase

FIG. 4. Enzymatic activities of mitochondrial respiratory chain and citrate synthase activity are decreased in isolated mitochondria from lumbar DRG of STZ-diabetic rats. Enzymatic activity of complex I was assessed as rotenone-sensitive portion of NADH-cytochrome c reductase (NCCR) ($n = 5$) (A), cytochrome c oxidase ($n = 6–7$) (B), and citrate synthase ($n = 5$) (C) and was measured as described in RESEARCH DESIGN AND METHODS. **Values are means ± SD, n = as indicated. *$P < 0.05$ vs. control (Ctrl) (unpaired Student's t test). Db, diabetic.**

control or 22-week STZ-diabetic rats was detected fluorometrically using the Amplex Red kit. ROS generation in lumbar DRG mitochondria in the presence of the substrates, pyruvate and malate, was not elevated in STZ-diabetic rats compared with control (Fig. 5G). However, when mitochondria samples were treated with antimycin A (a specific inhibitor of complex III), control rats significantly increased ROS production compared with age-matched STZ-diabetic rats (Fig. 5H). Finally, quantitative Western blotting showed diminished expression of some components of the mitochondrial electron transport chain (Fig. 6). NDUFS3 (component of complex I) and COX IV (component of complex IV) were significantly decreased by 50 and 20%, respectively, whereas levels of ATP synthase β-subunit and ERK remained unaltered.

DISCUSSION

In this study, we show, we believe for the first time, that mitochondrial respiratory function, activity, and expres-
sion of components of the respiratory chain and the Krebs cycle enzyme, citrate synthase, are decreased in DRG sensory neurons from rats with type 1 diabetes. This novel observation provides direct functional evidence of diabetes-induced alterations in mitochondrial performance at multiple sites along the mitochondrial respiratory chain. Previous studies have used only indirect assessments of mitochondrial inner-membrane polarization to analyze mitochondrial dysfunction in DRG sensory neurons in diabetes (17–19). Importantly, decreased mitochondrial respiratory activity was not associated with increased production of ROS. These observations imply that the diabetes-induced impairment of mitochondrial function is not associated with generation of oxidative stress.

Mitochondrial dysfunction has been proposed to mediate development of diabetes complications in endothelial cells, skeletal muscle, cardiomyocytes, and neurons (12–14,27). Studies of isolated endothelial cells demonstrate that a short period of exposure to high glucose concentrations induces hyperpolarization of the mitochondrial inner membrane, which is a consequence of glycolysis-driven enhancement of electron donation from the tricarboxylic acid pathway (5). It was therefore proposed that the high electrochemical potential difference across the mitochondrial membrane, driven by excessive proton gradient, prolonged the life of superoxide-producing electron transfer intermediates such as ubi-semiquinone (5). However, recent studies have revealed that respiration and enzymatic activities are decreased in mitochondria from hearts of STZ-diabetic rats (12,13), whereas several studies have reported decreased activity of the mitochondrial respiratory chain and the Krebs cycle enzyme, citrate synthase, in skeletal muscle of patients with type 2 diabetes (14–16). Our data are consistent with these findings and indicate that decreased rates of respiration and activities of mitochondrial complexes and citrate synthase occur in nervous tissues exposed to prolonged diabetes in vivo.

Diminished mitochondrial respiratory function caused by diabetes has been investigated by proteomic and gene array techniques (28,29). Reduced expression of oxidative phosphorylation genes have been found in type 2 diabetes (30), and decreased expression of the transcriptional regulator NRF-1 and the transcriptional coactivator peroxisome proliferator–activated receptor-γ coactivator 1α (PGC-1α) were observed in pre-diabetic and diabetic muscle (31). These proteins regulate cellular energy metabolism, including mitochondrial biogenesis and oxidative phosphorylation. Our results showing reduced expression of NDUFS3 and COX IV in Fig. 6 are consistent with these findings and support the suggestion that reduced activity of the mitochondrial respiratory chain could result from a proteome alteration leading to reduced expression/activity of a range of mitochondrial components.

Studies in lens (32), retina (33), and cardiac tissue (34) in experimental animal models of type 1 diabetes show that parts of glycolytic pathway function are depressed. In diabetic rats, activity of 6-phosphofructokinase is reduced in nerve (35), and activity of hexokinase, the first rate-limiting step in glycolysis, is reduced in DRG (36). Diminished activity of glycolytic pathway enzymes may combine to reduce delivery of pyruvate and other glucose metabolism-dependent products to the tricarboxylic acid pathway (32–34,37), and it has been shown that pool sizes of products of glycolysis, such as pyruvate, are either unchanged or reduced in diabetes (33,38). It therefore appears that rates of electron donation to the electron
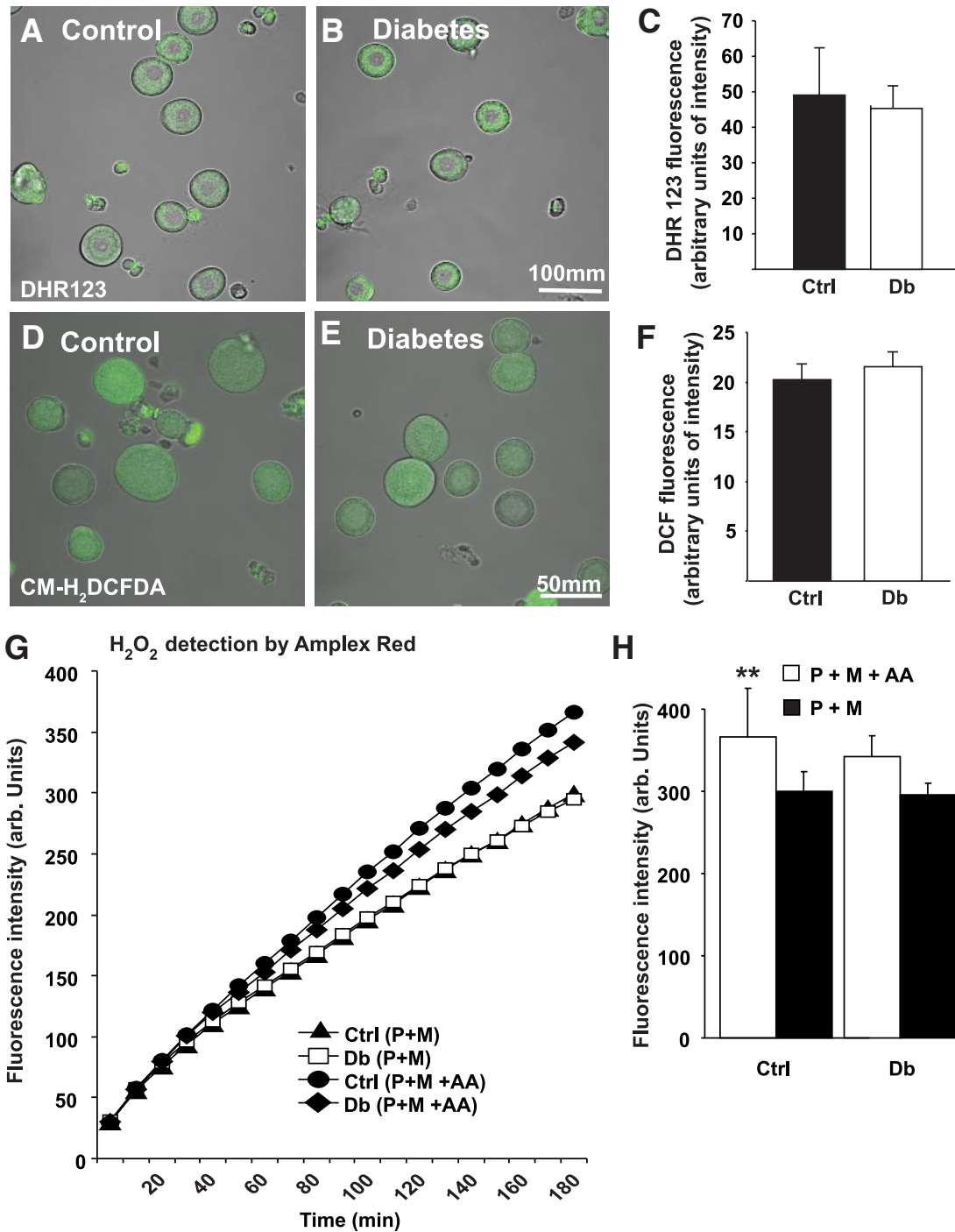
FIG. 5. ROS were not elevated in acutely isolated DRG sensory neurons or mitochondria from STZ-diabetic rats. *A–F*: ROS levels were assessed using real-time fluorescence imaging of DHR 123 or CM-H$_2$DCFDA. *A* and *B*: DHR 123 loaded neurons from acutely isolated lumbar DRG neurons of control or STZ-diabetic rats. Bar = 100 μm. *C*: Quantification of DHR 123 fluorescence intensities of neurons. Values are means ± SEM (n = 50–80 neurons, observed in five independently assessed control (Ctrl) and diabetic (Db) rats). *D* and *E*: CM-H$_2$DCFDA–based ROS imaging of sensory neurons from control and STZ-diabetic rats. Bar = 50 μm. *F*: Quantification of DCF fluorescence emission. Values are means ± SEM (n = 200–230 neurons, observed in two independently assessed control and diabetic rats). *G*: ROS generation is not elevated in isolated mitochondria from lumbar DRG of diabetic rats compared with control. Mitochondrial ROS generation was measured at state 4 with substrates pyruvate and malate (P + M) in the absence or presence of antimycin A (AA). H$_2$O$_2$ was measured fluorometrically in 0.1 mg/ml mitochondrial suspension with Amplex Red kits (50 μmol/l Amplex Red and 0.5 units/ml horseradish peroxidase). Values are mean with n = 5. *H*: Fluorescence intensity at 180 min. Significance level was determined by two-way ANOVA with Bonferroni's post hoc tests. **P < 0.01 for control (P + M) vs. control (P + M + AA). (A high-quality color representation of this figure is available in the online issue.)

transport chain are suboptimal in adult diabetic rats and may predispose to lower rates of mitochondrial respiratory chain activity and oxidative phosphorylation. Finally, a diabetes-induced rise in resting intracellular calcium to ≥200 nmol/l (39) can trigger elevated mitochondrial Ca^{2+} buffering by entry of Ca^{2+} through the Ca^{2+} uniporter and other routes, which can cause partial or complete inner mitochondrial membrane depolarization (27). There is evidence of aberrant mitochondrial buffering of calcium in neurons from diabetic rats. Plasma membrane depolariza-
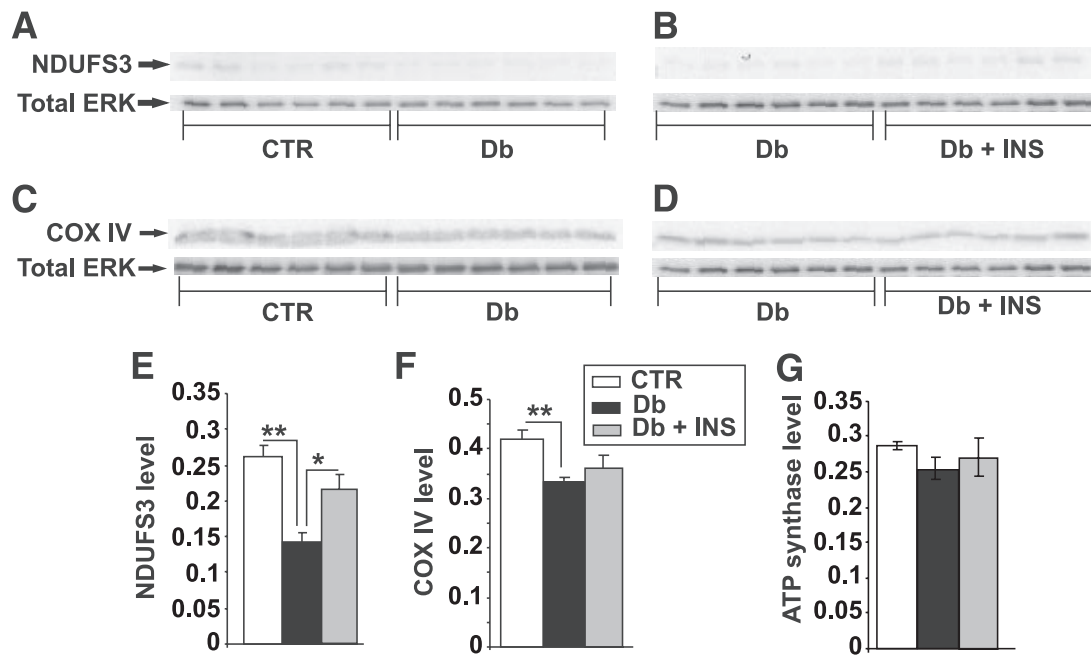
FIG. 6. Expression of components of the electron transport chain are reduced in DRG from STZ-diabetic rats. Shown are representative blots (A–D) and charts in which NDUFS3 (E), COX IV (F), and ATP synthase β subunit signal (G) have been presented relative to total ERK level. Values are the means ± SEM, n = 6. **P < 0.005 vs. control (CTR), *P < 0.05 vs. Db + INS (one-way ANOVA with Tukey's post hoc test). Db, diabetic; Db + INS, diabetic with insulin implant.

tion-induced Ca^{2+} transients are prolonged in diabetic neurons and blockade of mitochondrial uptake of Ca^{2+} using the mitochondrial uncoupler, CCCP, prevented these abnormalities (40). This implies, indirectly, that abnormal mitochondrial buffering of Ca^{2+} plays a role in shaping Ca^{2+} transients in diabetic neurons.

In our present study, impaired mitochondrial respiratory chain activity was not accompanied by increased ROS production in neuronal perikarya from STZ-diabetic rats, whereas generation of ROS in mitochondria from STZ-diabetic rats treated with pyruvate and malate in the presence of antimycin A was significantly decreased compared with control. In contrast, studies using cultures of embryonic sensory neurons showed that a high concentration of glucose directly triggers oxidative stress and apoptosis (8), suggesting differences in ROS production or management between embryonic and adult neurons in culture. We have recently found that ROS levels and adducts of 4-hydroxy-2-nonenal are elevated in the presence of high glucose in axons of adult sensory neurons isolated from 3- to 5-month STZ-diabetic rats, with the perikarya being unaffected (41). Oxidative damage to lipids in the sciatic nerve was increased in the present study, supporting previous work (9,42,43). These results suggest that mitochondrial function may differ between axons and perikarya or that oxidative stress in axons and other cells of the nerve trunk may derive from alternative sources.

Our studies were performed in rats that showed relatively mild STZ-induced diabetes, as indicated by maintenance of starting body weight over a long period of time. Marked hyperglycemia and increased A1C indicate that these rats were clearly diabetic and established biochemical consequences of hyperglycemia such as nerve polyol pathway flux (indicated by nerve fructose accumulation) and lipid peroxidation were present. This model contrasts with the acute and extreme STZ-induced insulin-deficient

diabetes frequently studied in rats and mice that may not adequately model long-term diabetes in well-managed patients. The absence of significantly reduced axonal caliber in myelinated fibers, altered thermal nociception, or loss of IENF after 22 weeks of diabetes confirms that STZ lacked direct neurotoxic effects and emphasizes the relatively mild nature of the diabetes in our rats, since all of these disorders have been widely reported in previous STZ-diabetic rodent studies. We do not suspect a lack of discrimination in our assays, as we have previously reported reduced axonal caliber (44), thermal hypoalgesia (25), and IENF loss (26) in STZ-diabetic rodents. Given that the rats in our present study showed marked hyperglycemia, polyol pathway flux, and lipid peroxidation, the data may suggest that additional risk factors may be required in concert with these established biochemical disorders to generate the indices of neuropathy described above.

Mitochondrial dysfunction appeared only after 16 weeks of diabetes and therefore represents a metabolic disorder of neurons that can emerge before onset of functional and structural manifestations of diabetic neuropathy. Interestingly, abnormalities in calcium homeostasis also appear after 8–12 weeks of diabetes and could possibly preempt mitochondrial dysfunction (39). The pathogenesis of this mitochondrial disorder may involve insulin deficiency per se, since our insulin treatment regime for the last month of diabetes had minimal effects on indices of systemic diabetes such as body weight, plasma, nerve sugar levels, lipid peroxidation, and A1C, but had marked effects on mitochondrial dysfunction. These findings agree with prior reports that insulin has direct effects on mitochondrial function (17,45). Insulin treatment also increased nerve total protein and IENF values above those of age-matched control rats, which may reflect the capacity of insulin to induce sensory neuron axonal sprouting (46,47). The contribution of impaired insulin signaling to complications of

both type 1 and type 2 diabetes, either independent of, or in concert with, hyperglycemia is clearly an area of emerging interest that deserves further study (11,46–48).

In conclusion, our data show that mitochondrial respiratory chain function and activity/expression of mitochondrial complexes as well as the Krebs cycle enzyme, citrate synthase, are decreased in mitochondria isolated from DRG of STZ-diabetic rats and can be normalized by insulin at levels that do not markedly alter the consequences of hyperglycemia. This decreased mitochondrial function does not induce ROS formation. The appearance of mitochondrial dysfunction at a time before onset of overt functional or structural neuropathy indicates the possibility of a pathogenic role for insulin deficiency in diabetic neuropathy that is independent of hyperglycemia.

REFERENCES

1. Yagihashi S. Pathogenetic mechanisms of diabetic neuropathy: lessons from animal models. J Peripher Nerv Syst 1997;2:113–132
2. Malik RA, Tesfaye S, Newrick PG, Walker D, Rajbhandari SM, Siddique I, Sharma AK, Boulton AJ, King RH, Thomas PK, Ward JD. Sural nerve pathology in diabetic patients with minimal but progressive neuropathy. Diabetologia 2005;48:578–585
3. Obrosova IG. Increased sorbitol pathway activity generates oxidative stress in tissue sites for diabetic complications. Antioxid Redox Signal 2005;7:1543–1552
4. Thornalley PJ. Glycation in diabetic neuropathy: characteristics, consequences, causes, and therapeutic options. Int Rev Neurobiol 2002;50:37–57
5. Nishikawa T, Edelstein D, Du XL, Yamagishi S, Matsumura T, Kaneda Y, Yorek MA, Beebe D, Oates PJ, Hammes HP, Giardino I, Brownlee M. Normalizing mitochondrial superoxide production blocks three pathways of hyperglycaemic damage. Nature 2000;404:787–790
6. Du XL, Edelstein D, Dimmeler S, Ju Q, Sui C, Brownlee M. Hyperglycemia inhibits endothelial nitric oxide synthase activity by posttranslational modification at the Akt site. J Clin Invest 2001;108:1341–1348
7. Calcutt NA, Cooper ME, Kern TS, Schmidt AM. Therapies for hyperglycaemia-induced diabetic complications: from animal models to clinical trials. Nat Rev Drug Discov 2009;8:417–429
8. Vincent AM, Russell JW, Low P, Feldman EL. Oxidative stress in the pathogenesis of diabetic neuropathy. Endocr Rev 2004;25:612–628
9. Yorek MA. The role of oxidative stress in diabetic vascular and neural disease. Free Radic Res 2003;37:471–480
10. Calcutt NA, Jolivalt CG, Fernyhough P. Growth factors as therapeutics for diabetic neuropathy. Curr Drug Targets 2008;9:47–59
11. Ishii DN. Implication of insulin-like growth factors in the pathogenesis of diabetic neuropathy. Brain Res Brain Res Rev 1995;20:47–67
12. Lashin OM, Szweda PA, Szweda LI, Romani AM. Decreased complex II respiration and HNE-modified SDH subunit in diabetic heart. Free Radic Biol Med 2006;40:886–896
13. Yang JY, Yeh HY, Lin K, Wang PH. Insulin stimulates Akt translocation to mitochondria: implications on dysregulation of mitochondrial oxidative phosphorylation in diabetic myocardium. J Mol Cell Cardiol 2009;46:919–926
14. Mogensen M, Sahlin K, Fernström M, Glintborg D, Vind BF, Beck-Nielsen H, Højlund K. Mitochondrial respiration is decreased in skeletal muscle of patients with type 2 diabetes. Diabetes 2007;56:1592–1599
15. Kruszynska YT, Mulford MI, Baloga J, Yu JG, Olefsky JM. Regulation of skeletal muscle hexokinase II by insulin in nondiabetic and NIDDM subjects. Diabetes 1998;47:1107–1113
16. Kelley DE, He J, Menshikova EV, Ritov VB. Dysfunction of mitochondria in human skeletal muscle in type 2 diabetes. Diabetes 2002;51:2944–2950
17. Huang TJ, Price SA, Chilton L, Calcutt NA, Tomlinson DR, Verkhratsky A, Fernyhough P. Insulin prevents depolarization of the mitochondrial inner membrane in sensory neurons of type 1 diabetic rats in the presence of sustained hyperglycemia. Diabetes 2003;52:2129–2136
18. Huang TJ, Sayers NM, Verkhratsky A, Fernyhough P. Neurotrophin-3 prevents mitochondrial dysfunction in sensory neurons of streptozotocin-diabetic rats. Exp Neurol 2005;194:279–283
19. Srinivasan S, Stevens M, Wiley JW. Diabetic peripheral neuropathy: evidence for apoptosis and associated mitochondrial dysfunction. Diabetes 2000;49:1932–1938
20. Calcutt NA, Lopez VL, Bautista AD, Mizisin LM, Torres BR, Shroads AL, Mizisin AP, Stacpoole PW. Peripheral neuropathy in rats exposed to dichloroacetate. J Neuropathol Exp Neurol 2009;68:985–993
21. Frezza C, Cipolat S, Scorrano L. Organelle isolation: functional mitochondria from mouse liver, muscle and cultured fibroblasts. Nat Protoc 2007;2:287–295
22. Chowdhury SK, Gemin A, Singh G. High activity of mitochondrial glycerophosphate dehydrogenase and glycerophosphate-dependent ROS production in prostate cancer cell lines. Biochem Biophys Res Commun 2005;333:1139–1145
23. Chowdhury SK, Drahota Z, Floryk D, Calda P, Houstek J. Activities of mitochondrial oxidative phosphorylation enzymes in cultured amniocytes. Clin Chim Acta 2000;298:157–173
24. Chowdhury SK, Raha S, Tarnopolsky MA, Singh G. Increased expression of mitochondrial glycerophosphate dehydrogenase and antioxidant enzymes in prostate cancer cell lines/cancer. Free Radic Res 2007;41:1116–1124
25. Calcutt NA, Freshwater JD, Mizisin AP. Prevention of sensory disorders in diabetic Sprague-Dawley rats by aldose reductase inhibition or treatment with ciliary neurotrophic factor. Diabetologia 2004;47:718–724
26. Beiswenger KK, Calcutt NA, Mizisin AP. Dissociation of thermal hypoalgesia and epidermal denervation in streptozotocin-diabetic mice. Neurosci Lett 2008;442:267–272
27. Verkhratsky A, Fernyhough P. Mitochondrial malfunction and Ca2+ dyshomeostasis drive neuronal pathology in diabetes. Cell Calcium 2008;44:112–122
28. Bugger H, Abel ED. Molecular mechanisms for myocardial mitochondrial dysfunction in the metabolic syndrome. Clin Sci (Lond) 2008;114:195–210
29. Bugger H, Chen D, Riehle C, Soto J, Theobald HA, Hu XX, Ganesan B, Weimer BC, Abel ED. Tissue-specific remodeling of the mitochondrial proteome in type 1 diabetic Akita mice. Diabetes 2009;58:1986–1997
30. Mootha VK, Lindgren CM, Eriksson KF, Subramanian A, Sihag S, Lehar J, Puigserver P, Carlsson E, Ridderstråle M, Laurila E, Houstis N, Daly MJ, Patterson N, Mesirov JP, Golub TR, Tamayo P, Spiegelman B, Lander ES, Hirschhorn JN, Altshuler D, Groop LC. PGC-1alpha-responsive genes involved in oxidative phosphorylation are coordinately downregulated in human diabetes. Nat Genet 2003;34:267–273
31. Patti ME, Butte AJ, Crunkhorn S, Cusi K, Berria R, Kashyap S, Miyazaki Y, Kohane I, Costello M, Saccone R, Landaker EJ, Goldfine AB, Mun E, DeFronzo R, Finlayson J, Kahn CR, Mandarino LJ. Coordinated reduction of genes of oxidative metabolism in humans with insulin resistance and diabetes: Potential role of PGC1 and NRF1. Proc Natl Acad Sci U S A 2003;100:8466–8471
32. Obrosova I, Faller A, Burgan J, Ostrow E, Williamson JR. Glycolytic pathway, redox state of NAD(P)-couples and energy metabolism in lens in galactose-fed rats: effect of an aldose reductase inhibitor. Curr Eye Res 1997;16:34–43
33. Ola MS, Berkich DA, Xu Y, King MT, Gardner TW, Simpson I, LaNoue KF. Analysis of glucose metabolism in diabetic rat retinas. Am J Physiol Endocrinol Metab 2006;290:E1057–E1067
34. Trueblood N, Ramasamy R. Aldose reductase inhibition improves altered glucose metabolism of isolated diabetic rat hearts. Am J Physiol 1998;275:H75–H83
35. Calcutt NA, Tomlinson DR, Willars GB. Ganglioside treatment of streptozotocin-diabetic rats prevents defective axonal transport of 6-phosphofructokinase activity. J Neurochem 1988;50:1478–1483
36. Gardiner NJ, Wang Z, Luke C, Gott A, Price SA, Fernyhough P. Expression

of hexokinase isoforms in the dorsal root ganglion of the adult rat and effect of experimental diabetes. Brain Res 2007;1175:143–154

37. Stanley WC, Lopaschuk GD, McCormack JG. Regulation of energy substrate metabolism in the diabetic heart. Cardiovasc Res 1997;34:25–33

38. Li F, Szabó C, Pacher P, Southan GJ, Abatan OI, Charniauskaya T, Stevens MJ, Obrosova IG. Evaluation of orally active poly(ADP-ribose) polymerase inhibitor in streptozotocin-diabetic rat model of early peripheral neuropathy. Diabetologia 2004;47:710–717

39. Huang TJ, Sayers NM, Fernyhough P, Verkhratsky A. Diabetes-induced alterations in calcium homeostasis in sensory neurones of streptozotocin-diabetic rats are restricted to lumbar ganglia and are prevented by neurotrophin-3. Diabetologia 2002;45:560–570

40. Kostyuk E, Svichar N, Shishkin V, Kostyuk P. Role of mitochondrial dysfunction in calcium signalling alterations in dorsal root ganglion neurons of mice with experimentally-induced diabetes. Neuroscience 1999;90:535–541

41. Zherebitskaya E, Akude E, Smith DR, Fernyhough P. Development of selective axonopathy in adult sensory neurons isolated from diabetic rats: role of glucose-induced oxidative stress. Diabetes 2009;58:1356–1364

42. Coppey LJ, Gellett JS, Davidson EP, Yorek MA. Preventing superoxide formation in epineurial arterioles of the sciatic nerve from diabetic rats restores endothelium-dependent vasodilation. Free Radic Res 2003;37:33–40

43. Obrosova IG, Pacher P, Szabó C, Zsengeller Z, Hirooka H, Stevens MJ, Yorek MA. Aldose reductase inhibition counteracts oxidative-nitrosative stress and poly(ADP-ribose) polymerase activation in tissue sites for diabetes complications. Diabetes 2005;54:234–242

44. Calcutt NA, Campana WM, Eskeland NL, Mohiuddin L, Dines KC, Mizisin AP, O'Brien JS. Prosaposin gene expression and the efficacy of a prosaposin-derived peptide in preventing structural and functional disorders of peripheral nerve in diabetic rats. J Neuropathol Exp Neurol 1999;58:628–636

45. Huang TJ, Verkhratsky A, Fernyhough P. Insulin enhances mitochondrial inner membrane potential and increases ATP levels through phosphoinositide 3-kinase in adult sensory neurons. Mol Cell Neurosci 2005;28:42–54

46. Toth C, Brussee V, Martinez JA, McDonald D, Cunningham FA, Zochodne DW. Rescue and regeneration of injured peripheral nerve axons by intrathecal insulin. Neuroscience 2006;139:429–449

47. Toth C, Brussee V, Zochodne DW. Remote neurotrophic support of epidermal nerve fibres in experimental diabetes. Diabetologia 2006;49:1081–1088

48. Sima AA. Pathological mechanisms involved in diabetic neuropathy: can we slow the process? Curr Opin Investig Drugs 2006;7:324–337